



Anthropogenic Fine Particulate Matter Pollution Will Be Exacerbated in Eastern China Due to 21st-Century GHG Warming

³ Huopo Chen^{1, 2*}, Huijun Wang^{2, 1}, Jianqi Sun^{1, 2}, Yangyang Xu³, and Zhicong Yin²

⁴ ¹ *Nansen-Zhu International Research Centre, Institute of Atmospheric Physics,*
⁵ *Chinese Academy of Sciences, Beijing, China*

² Collaborative Innovation Center on Forecast and Evaluation of Meteorological Disasters, Nanjing University for Information Science and Technology, Nanjing,

8 *China*
9 ³*Department of Atmospheric Sciences, Texas A&M University, College Station Texas,*
10 *USA*

— 2 — **Comments by the Human-Computer Committee**

16 Email: chenhuopo@mail.iap.ac.cn

17 Tel: (+86)010-82995057



19 Abstract

20 China has experienced a substantial increase in severe haze events over the past
21 several decades, which is primarily attributed to the increased pollutant emissions
22 caused by its rapid economic development. The climate changes observed under the
23 warming scenarios, especially those induced by increases in greenhouse gases (GHG),
24 are also conducive to the increase in air pollution. However, how the air pollution
25 changes in response to the GHG warming has not been thoroughly elucidated to date.
26 We investigate this change using the century-long large ensemble simulations with the
27 Community Earth System Model 1 (CESM1) with the fixed anthropogenic emissions
28 at the year 2005. Our results show that although the aerosol emission is assumed to be
29 a constant throughout the experiment, anthropogenic air pollution presents robust
30 positive responses to the GHG-induced warming, with an increase of approximately
31 68% to be observed in the most severe days at the end of the 21st century. Further
32 research indicates that the increased stagnation days and the decreased light
33 precipitation days are the primary causes of the increase in PM_{2.5} concentration, as
34 well as the anthropogenic air pollution days. Estimation shows that the effect of
35 climate change induced by the GHG warming can account for 11%-28% of the
36 changes in anthropogenic air pollution days over eastern China. Therefore, in the
37 future, more stringent regulations on regional air pollution emissions are needed to
38 balance the effect from climate change.

39



40 1. Introduction

41 The extraordinarily rapid development of China has caused extremely high
42 aerosol loading and gaseous pollutant emissions that have enveloped most regions
43 across China in the recent decades. The increased pollutant emissions, particularly for
44 the particulate matter finer than 2.5 μm in aerodynamic diameter ($\text{PM}_{2.5}$), generally
45 result in severe haze events and present a major threat to public health (Gao et al.,
46 2017; Tang et al., 2017; Wang, 2018), crop production (Tie et al., 2016), and regional
47 climates (Cao et al., 2016). For example, the annual averaged $\text{PM}_{2.5}$ in Beijing
48 exceeded 75 $\mu\text{g}/\text{m}^3$ during 2009-2016 (Fig. 1b), which more than three times the
49 recommended 24-hour standard (25 $\mu\text{g}/\text{m}^3$) of the World Health Organization (WHO).
50 This degeneration of the air pollution across China, which is similar to that in Beijing,
51 is primarily caused by the integrated effects of high emissions and poor ventilation
52 (Chen and Wang, 2015; Zhang et al., 2016a). Many efforts are thus underway to
53 reduce emissions that cause severe haze pollutions. However, the question remains of
54 whether climate change will offset or facilitate these efforts.

55 Recent studies have documented that the exacerbation of air quality over eastern
56 China was partly modulated by meteorological conditions and climate variability that
57 are generally conducive to the severe haze occurrences (Li et al., 2018; Liao and
58 Chang, 2014; Wang and Chen, 2016; Yang et al., 2016; Zhang et al., 2014; Zhang et
59 al., 2016b). Specifically, Wang *et al.* (2015) revealed that the shrinking Arctic sea ice
60 favors less cyclone activity and a more stable atmosphere conducive to haze
61 formation, which can explain approximately 45%-67% of the interannual to



62 interdecadal variability of winter haze days over eastern China. Besides Arctic sea ice,
63 other decadal variability and changes, including weak East Asian winter monsoon
64 (Jeong et al., 2017; Li et al., 2016; Yin et al., 2015), strong El Niño-Southern
65 oscillation (Gao and Li, 2015; Zhao et al., 2018), high Pacific decadal oscillation
66 (Zhao et al., 2016), and high Arctic oscillation (Cai et al., 2017), may have contributed.

67 In addition, the increasing winter haze days over eastern China may also be linked to
68 the low boundary layer height (Huang et al., 2018; Wang et al., 2018), weakened
69 northerly winds (Yang et al., 2017), decreased relative humidity (Ding and Liu, 2014),
70 and increased sea surface temperature (Xiao et al., 2015; Yin and Wang, 2016; Yin et
71 al., 2017).

72 Global warming generally presents an adverse impact on the haze pollution
73 across China. Simulations of the dynamic downscaling by the regional climate model
74 RegCM4 under the RCP4.5 (Representative Concentration Pathway) scenarios have
75 shown that the air environment carrying capacity tends to decrease, and the weak
76 ventilation days tend to increase, in the 21st century across China, suggesting an
77 increase in the haze pollution potential compared to the current state (Han et al., 2017).

78 Furthermore, Cai *et al.* (2017) projected that the days conducive to severe haze
79 pollution in Beijing would increase by 50% at the end of the 21st century (2050-2099)
80 under the RCP8.5 scenarios compared to the historical period.

81 These qualitative estimations of the haze pollution response to climate changes
82 generally derived from the *potential* changes of the corresponding meteorological
83 conditions indirectly. No studies to date quantitatively assessed the simulated PM



84 directly. How the fine particulate matter pollution changes in response to the global
85 warming in China has not been thoroughly elucidated to date. This study particularly
86 focuses on the anthropogenic PM_{2.5} loading and its response to the future warming. In
87 this study, the large ensemble simulations from the Community Earth System Model
88 Version 1 (CESM1) throughout the 21st century that are induced by increasing
89 greenhouse gases (GHG) emissions along the trajectory RCP8.5 but retaining the
90 emissions of aerosols and/or their precursors fixed at the year of 2005 level
91 (RCP8.5_FixAerosol2005; Xu and Lamarque, 2018) will be utilized.

92 **2. Data and methods**

93 **2.1 PM_{2.5} observational datasets**

94 Surface hourly PM_{2.5} concentration data released since 2013 are taken from the
95 website of the Ministry of Environmental Protection (<http://106.37.208.233:20035>),
96 which covers 1602 sites across China. The duration of available datasets varies across
97 sites because of the gradual development of the monitoring network in recent years. In
98 our study region of eastern China (east to 100 °E), there are 1263 sites remaining after
99 the sites with missing values were removed during 2015-2017. Additionally, surface
100 daily PM_{2.5} concentrations for the Beijing, Shanghai, Guangzhou, and Chengdu cities
101 that had relatively longer monitoring times are also collected from the U.S. Beijing
102 Embassy (<http://www.stateair.net/web/historical/1/1.html>).

103 **2.2 CESM1 model simulations**

104 The CESM1 is an Earth system model involving the atmosphere, land, ocean,



105 and sea-ice components with a nominal 1 ° by 1 ° horizontal resolution (Hurrell et al.,
106 2013). The RCP8.5_FixAerosol2005 simulations are forced by the RCP8.5 scenario,
107 but all emissions of sulfate (SO_4), black carbon (BC) and primary organic matter
108 (POM), and secondary organic aerosols (SOA; or their precursors) and atmospheric
109 oxidants are fixed at the present-day level (2005). These simulations include 16
110 ensemble members, differing solely in their atmospheric initial conditions with a tiny
111 random temperature difference (order of 10^{-14} °C; Kay et al., 2015). Using this
112 relatively large ensemble can substantially reduce the contribution of natural
113 variability of the climate system to the result estimation (Xu and Lamarque, 2018).

114 For the aerosol emission in the RCP scenarios database, just its decadal change is
115 considered rather than the emission at a single year (Lamarque et al., 2011). Here, the
116 years of 2006-2015 are considered as the reference period in the
117 RCP8.5_FixAerosol2005 simulations. The differences of the mean climates from the
118 reference period are largely due to the increase in GHG emissions and are not
119 attributed to the decline in aerosol emissions, as specified in RCP8.5. The changes of
120 anthropogenic PM_{2.5} loadings and anthropogenic air pollution days in our study are
121 thus only a result of the GHG-induced climate change, rather than changes in aerosol
122 emission. Note that just four species of PM_{2.5} components that show a substantial
123 threat to public health are considered here for analysis, including SO₄, BC, POM, and
124 SOA from the CESM1 simulations.

125 **2.3 Definition of the fraction of attributable risk**

126 The influences of the GHG-induced climate changes on the anthropogenic air



127 pollutions in China are investigated using the metric of the fraction of attributable risk
128 (FAR), which has been widely used for attribute analyses of climate extreme changes
129 (Chen and Sun, 2017; Stott et al., 2004). FAR is defined as the $1-P_0/P_I$, where P_0 is
130 the probability of exceeding a certain threshold during the reference period and P_I is
131 the probability exceeding the same threshold during a given period. FAR thus presents
132 the quantitative estimations of effects of the GHG-induced climate changes on the
133 anthropogenic air pollutions.

134 **2.4 Definition of stagnation days**

135 The changes of the stagnation days that were induced by the increase of GHG
136 emissions are also evaluated in our study to explore the possible impact of climate
137 change on the anthropogenic air pollutions. The day is considered to be stagnant when
138 the daily mean near-surface wind speed is less than 3.2 m/s, the daily mean 500-hPa
139 wind speed is less than 13 m/s, and the daily accumulated precipitation is less than 1
140 mm (Horton et al., 2012).

141 **3. Results**

142 **3.1 Observational changes in PM_{2.5} pollutions**

143 The days of severe haze pollution increased over the past several decades across
144 eastern China, particularly for the episodes of January 2013, December 2015, and
145 December 2016, when several severe haze alerts were reached. High PM_{2.5} loading
146 was centralized over the Jing-Jin-Ji (JJJ) region, Shangdong, and Henan provinces, as
147 well as the Sichuan Basin (Fig. 1a). The annual mean PM_{2.5} mass concentrations for



148 most sites over these regions exceed $75 \mu\text{g}/\text{m}^3$. According to the statistics, there are
149 approximately 95% sites where the annual mean $\text{PM}_{2.5}$ concentration exceeded the
150 WHO recommended 24-hour standard ($25 \mu\text{g}/\text{m}^3$) across eastern China, and there are
151 65 sites centralized by Beijing, where the annual mean $\text{PM}_{2.5}$ concentration was larger
152 than $75 \mu\text{g}/\text{m}^3$, which would present the possibility of exposing people to serious
153 health hazards (World Health Organization, 2014).

154 Regarding the four economic zones of Beijing, Shanghai, Guangzhou, and
155 Chengdu cities over China, serious $\text{PM}_{2.5}$ pollution can be expected in recent years,
156 especially for the Beijing and Chengdu regions (Fig. 1). Taking Beijing as an example,
157 the annual mean $\text{PM}_{2.5}$ concentration was stably exceeding $100 \mu\text{g}/\text{m}^3$, and more than
158 a half of the year had experienced severe air pollution ($> 75 \mu\text{g}/\text{m}^3$) before 2013.
159 Since 2013, China's State Council released its Air Pollution Prevention and Control
160 Action Plan, which requires the key regions, including the JJJ, the Yangtze River
161 Delta (YRD), and the Pearl River Delta (PRD) to reduce their atmospheric levels of
162 $\text{PM}_{2.5}$ by 25%, 20%, and 15%, respectively, by the end of year 2017 (State Council,
163 2013). Effort is obvious, and the $\text{PM}_{2.5}$ loading and the air pollution days present
164 sharp decreases in recent years. However, the strict emission policies substantially
165 cost the economic development, which cannot meet the current requirement of the
166 rapid development of China. Thus, scientifically quantifying the roles of
167 anthropogenic emissions and climate changes shows great importance for seeking the
168 balance between socioeconomic development and emission reduction.

169 **3.2 Simulated changes in anthropogenic $\text{PM}_{2.5}$ pollutions**



170 A strong correlation (0.69) is found for the annual mean PM_{2.5} concentration
171 between the observation and median ensemble of CESM1 simulations over eastern
172 China (Fig. S1). The high concentrations across eastern China, including the regions
173 centralized by Beijing and Chengdu, are reasonably reproduced. However, a negative
174 bias is obvious, primarily because only four major species are considered in this study
175 from the CESM1 simulations.

176 The median ensemble-mean change of the PM_{2.5} surface concentration presents
177 strong regional dependence across China with significantly decreasing trends over the
178 southeastern part of eastern China and significantly increasing trends over the other
179 regions throughout the 21st century (Fig. S2), even though the emissions are constant
180 throughout the experiment. The regional differences in the total PM_{2.5} changes are
181 mainly due to SO₄, which can account for approximately 50% of the total PM_{2.5} mass
182 (Xu and Lamarque, 2018). The species of BC and POM are reported to significantly
183 increase in the 21st century across eastern China, although the aerosol emissions were
184 fixed at the level in 2005. Figure 2 presents the simulated PM_{2.5} loadings from the
185 CESM1 model, in terms of column burden and surface concentration, are significantly
186 increasing throughout the 21st century. The increase in the total PM_{2.5} is
187 approximately 8% for the column burden and 2% for the surface concentration at the
188 end of the 21st century (2090-2099) with respect to the current state (2006-2015).
189 These increasing trends of PM_{2.5} loadings are mainly due to the significant increases
190 of the major PM_{2.5} species, except for SOA, in which the surface concentration
191 presents a slight decrease. Furthermore, the increases of all major PM_{2.5} species in



192 terms of column burden (BC: 11%, SO₄: 6%, SOA: 11%, and POM: 11%) show
193 stronger than the surface concentration (BC: 4%, SO₄: 2%, SOA: -1%, and POM:
194 4%).

195 As mentioned above, the PM_{2.5} surface concentration in the two economic zones
196 of YRD and PRD present a negative response to the GHG-induced warming, while
197 the corresponding column burden shows significantly increasing trends (Fig. S3). The
198 decreases of the surface concentration over these two zones are primarily contributed
199 by the changes of SO₄ and SOA, while there are no obvious trends for BC and POM
200 (Figs. S4-S7). The robust response of the increased surface wind speed and decreased
201 upper-level wind speed to GHG warming can be partly responsible for the changes of
202 the major PM_{2.5} species in these two zones, which will be further discussed. Over the
203 zones of JJJ and SC, the major PM_{2.5} species present the significantly rising trends
204 throughout the 21st century. For the surface concentration, BC is reported to increase
205 by 4% and 8% for JJJ and SC, respectively, at the end of the 21st century. The other
206 species, such as SO₄ and POM, increase by 4% and 4%, respectively, in the JJJ
207 regions and by 2% and 9%, respectively, in SC regions. Relatively stronger responses
208 can be seen in changes of the column burden for all major species (Figs. S4-S7). The
209 increased concentrations of PM_{2.5} species finally result in significantly increasing
210 trends of the total PM_{2.5} loading over these two regions, which will present a more
211 direct effect on human health.

212 The increase in PM_{2.5} surface concentration throughout the 21st century
213 substantially leads to the significant increase of the light anthropogenic PM_{2.5}



214 pollution days ($\text{PM}_{2.5} > 25 \mu\text{g}/\text{m}^3$) across the northwestern part of eastern China (Fig.
215 S8). Due to the decrease of $\text{PM}_{2.5}$ concentration over the southeastern part of eastern
216 China, the light anthropogenic air pollution days can be expected to decrease in this
217 region. However, the severe anthropogenic air pollution days ($\text{PM}_{2.5} > 75 \mu\text{g}/\text{m}^3$)
218 show a robust positive response to the GHG-induced warming across eastern China,
219 particularly for the regions in which the high $\text{PM}_{2.5}$ concentration was localized (Fig.
220 3). The increase of the severe anthropogenic air pollution days is considerably
221 stronger than the light air pollution days, with an increase of approximately 68% to be
222 observed at the end of 21st century, while an increase of 3% is expected for the light
223 air pollution days over eastern China.

224 **3.3 Attributable changes due to GHG warming**

225 Although the aerosol emission was constant throughout the experiment, our
226 study reveals that the $\text{PM}_{2.5}$ loadings and their associated pollution days still present
227 significant increases throughout the 21st century, primarily resulting from the impact
228 of climate change induced by GHG warming. One may ask how large a contribution
229 the climate change exerts on the changes in anthropogenic air pollution. To
230 quantitatively address this issue, the framework of the “Fraction of Attributable Risk
231 (FAR)” that has been widely used for attribute analyses of climate extreme changes
232 (Chen and Sun, 2017; Stott et al., 2004) is employed in this study.

233 Figure 4 shows the percentage changes of the anthropogenic air pollution days
234 throughout the 21st century over eastern China and their associated FAR variations.
235 The regional averaged anthropogenic air pollution days present a significant increase



236 in the 21st century as addressed above. Correspondingly, synchronous increasing
237 trends can be found in FAR for both light and severe anthropogenic air pollution days.
238 For the light pollution days, FAR is estimated to be 28% at the end of the 21st century,
239 implying that approximately 28% of the pollution days are contributed by the climate
240 change that was induced by GHG warming. For the severe pollution days, FAR shows
241 a relatively smaller value of approximately 11%. Furthermore, the high FAR values
242 are mainly located over the regions of high PM_{2.5} loadings concentrated over eastern
243 China, suggesting considerably stronger effects of climate changes in this study. Note
244 that the FAR values estimated in this research may be underestimated because the
245 GHG-induced warming impact was involved in the selected reference period that
246 resulted in the overestimation of the probability of anthropogenic air pollution days.

247 **3.4 Effects of the changes in meteorological conditions**

248 We further examined the changes of meteorological conditions induced by the
249 GHG warming that alternatively exerted effects on air pollution. Our results show that
250 the local boundary layer height presents as higher under the warming scenario (Fig.
251 5a), which benefits the vertical transport of the air pollutant.

252 However, a robust negative response of the horizontal advection to the
253 GHG-induced warming across eastern China can be found in the troposphere (Fig. 5b,
254 c), facilitating air pollutant accumulation. The change of surface wind speed in
255 response to the GHG warming is highly similar with the variation of PM_{2.5} surface
256 concentration, with wind speed increasing in the southeastern part of eastern China
257 and decreasing in the northwestern part. Variations of surface wind speeds are thus



258 mainly responsible for the changes of PM_{2.5} surface concentration over eastern China.

259 Different responses can be found for the tropospheric upper-level wind speeds, which
260 are reported to substantially decrease. These decreases would directly result in
261 significant increases of the stagnation days over eastern China, particularly over the
262 northern and SC basin (Fig. 6).

263 In response to the GHG-induced warming, the stagnation days over eastern
264 China are estimated to increase by 6% at the end of 21st century with respect to the
265 current period. For the specific economic zones, the stagnation days over the SC and
266 JJJ regions show considerably stronger rising trends, while relatively weaker increases
267 are observed over the YRD and PRD regions. The number of stagnation days is
268 estimated to increase by 13% and 6% at the end of the 21st century for the SC and JJJ
269 regions, respectively. Briefly, though the atmospheric stratification appears to be
270 considerably more unstable in response to the GHG warming, the weakened
271 horizontal advection would substantially increase the stagnation days over eastern
272 China, which provides a beneficial background for the air pollutant accumulation and
273 further increases the occurrence probability of the anthropogenic air pollution events.

274 Early studies have documented a significant increase in total precipitation across
275 China due to the GHG-induced warming (Chen, 2013; Li et al., 2018; Wang et al.,
276 2012), which seems to represent a conflict with the increase of the anthropogenic air
277 pollution days. To resolve this issue, the precipitation changes in terms of light
278 precipitation days (daily accumulated precipitation < 10 mm) and heavy precipitation
279 days (> 10 mm) are further examined (Fig. 5d, e). Clearly, the heavy precipitation



280 days present an increase, while the light precipitation days show a decrease, across
281 eastern China in response to the warming. Though the precipitation shifts toward
282 heavy precipitation events, its cleansing impact on air pollutants has not increased
283 because an increase in heavy precipitation days appears to be insufficient to further
284 enhance the wet removal ability (Xu and Lamarque, 2018). In contrast, the decrease in
285 light precipitation days substantially weakens the wet deposition of air pollutants,
286 leading to the increase of the PM_{2.5} loading, as well as anthropogenic air pollution
287 days.

288 **4. Conclusions**

289 The world is predicted to experience increased disasters, such as heat waves,
290 flash floods, and storms, due to the continuous global warming induced by the GHG
291 increase. The research question we aim to address in this study is how the GHG
292 warming would affect the anthropogenic PM_{2.5} pollutions across China. Our
293 evaluations show that the anthropogenic PM_{2.5} loadings, as well as the anthropogenic
294 PM_{2.5} pollution days, would substantially increase under the global warming
295 conditions even the aerosol emissions fixed at current levels. More stringent
296 regulations are thus suggested for regional aerosol emissions to maintain the air
297 quality standard as the current state.

298 The climate changes induced by GHG warming exert their effects on the
299 anthropogenic air pollutions across eastern China via two ways that are of interest in
300 this study. First, the weakened tropospheric wind speed induced by the GHG warming
301 would result in a decrease of the horizontal advection and lead to an increase in the



302 number of stagnation days, facilitating the local accumulation of air pollutants.
303 Second, the number of light precipitation days would decrease due to GHG-induced
304 warming, although the total precipitation would clearly increase across China. This
305 shift toward more no-rainfall days would further weaken the wet deposition of PM_{2.5}
306 pollutants. Of course, under the warming scenarios, a large discrepancy exists among
307 the different meteorological processes that benefit the air pollutions at the current
308 state, leading to the fuzzy recognition of air pollution change. For example, the
309 boundary layer height shows an increase in response to the GHG warming that may
310 strengthen the vertical dissipation of air pollutants. Thus, more studies are suggested
311 in the future to further understand the mechanisms governing air quality across China.
312
313



314 **Author contributions**

315 H. P. Chen and H. J. Wang designed the research; H. P. Chen analyzed the data.

316 All the authors discussed the results and wrote the paper.

317

318 **Competing interests**

319 The authors declare that they have no conflict of interest.

320

321 **Acknowledgements**

322 This work is jointly supported by the National Natural Science Foundation of

323 China (Grant No: 41421004), the National Key Research and Development Program

324 of China (Grant No: 2016YFA0600701), and the CAS-PKU Joint Research Program.

325



326 References

- 327 Cai, W. J., Li, K., Liao, H., Wang, H. J., and Wu, L. X.: Weather conditions conducive
328 to Beijing severe haze more frequent under climate change, *Nature Climate
329 Change*, 7, 257-263, 2017.
- 330 Cao, C., Lee, X. H., Liu, S. D., Schultz, N., Xiao, W., Zhang, M., and Zhao, L.: Urban
331 heat islands in China enhanced by haze pollution, *Nature Communications*, 7,
332 12509, 2016.
- 333 Chen, H. P.: Projected change in extreme rainfall events in China by the end of the
334 21st century using CMIP5 models, *Chin. Sci. Bull.*, 58, 1462-1472, 2013.
- 335 Chen, H. P. and Sun, J. Q.: Contribution of human influence to increased daily
336 precipitation extremes over China, *Geophys. Res. Lett.*, 44, 2436-2444, 2017.
- 337 Chen, H. P. and Wang, H. J.: Haze days in North China and the associated
338 atmospheric circulations based on daily visibility data from 1960 to 2012, *J.
339 Geophys. Res. Atmos.*, 120, 5895-5909, 2015.
- 340 Ding, Y. H. and Liu, Y. J.: Analysis of long-term variations of fog and haze in China
341 in recent 50 years and their relations with atmospheric humidity, *Sci. China Earth
342 Sci.*, 57, 36-46, 2014.
- 343 Gao, H. and Li, X.: Influences of El Niño Southern Oscillation events on haze
344 frequency in eastern China during boreal winters, *Int. J. Climatol.*, 35, 2682-2688,
345 2015.
- 346 Gao, J. H., Woodward, A., Vardoulakis, S., Kovats, S., Wilkinson, P., Li, L. P., Xu, L.,
347 Li, J., Yang, J., Li, J., Cao, L., Liu, X. B., Wu, H. X., and Liu, Q. Y.: Haze, public



- 348 health and mitigation measures in China: A review of the current evidence for
349 further policy response, *Sci. Total Environ.*, 578, 148-157, 2017.
- 350 Han, Z. Y., Zhou, B. T., Xu, Y., Wu, J., and Shi, Y.: Projected changes in haze
351 pollution potential in China: an ensemble of regional climate model simulations,
352 *Atmos. Chem. Phys.*, 17, 10109-10123, 2017.
- 353 Horton, D. E., Harshvardhan, and Diffenbaugh, N. S.: Response of air stagnation
354 frequency to anthropogenically enhanced radiative forcing, *Environ. Res. Lett.*, 7,
355 044034, 2012.
- 356 Huang, Q., Cai, X., Wang, J., Song, Y., and Zhu, T.: Climatological study of the
357 boundary-layer air stagnation index for China and its relationship with air
358 pollution, *Atmos. Chem. Phys.*, 18, 7573-7593, 2018.
- 359 Hurrell, J. W., Holland, M. M., Gent, P. R., Ghan, S., Kay, J. E., Kushner, P. J.,
360 Lamarque, J. F., Large, W. G., Lawrence, D., Lindsay, K., Lipscomb, W. H.,
361 Long, M. C., Mahowald, N., Marsh, D. R., Neale, R. B., Rasch, P., Vavrus, S.,
362 Vertenstein, M., Bader, D., Collins, W. D., Hack, J. J., Kiehl, J., Marshall, S.: The
363 community earth system model: A framework for collaborative research, *Bull.*
364 *Amer. Meteorol. Soc.*, 94(9), 1339-1360, 2013.
- 365 Jeong, J. I. and Park, R. J.: Winter monsoon variability and its impact on aerosol
366 concentrations in East Asia, *Environ. Pollution*, 221, 285-292, 2017.
- 367 Kay, J. E., Deser, C., Phillips, A., Mai, A., Hannay, C., Strand, G., Arblaster, J. M.,
368 Bates, S. C., Danabasoglu, G., Edwards, J., Holland, M., Kushner, P., Lamarque,
369 J. F., Lawrence, D., Lindsay, K., Middleton, A., Munoz, E., Neale, R., Oleson, K.,



- 370 Polvani, L., and Vertenstein, M.: The community earth system model (CESM)
371 large ensemble project: A community resource for studying climate change in the
372 presence of internal climate variability, Bull. Amer. Meteorol. Soc., 96(8),
373 1333-1349, 2015.
- 374 Lamarque, J. F., Kyle, P. P., Meinshausen, M., Riahi, K., Smith, S. J., van Vuuren, D.
375 P., Conley, A. J., and Vitt, F.: Global and region evolution of short-lived
376 radiatively-active gases and aerosols in the Representative Concentration
377 Pathway, Climatic Change, 109(1), 191-212, 2011.
- 378 Li, H. X., Chen, H. P., Wang, H. J., and Yu, E. T.: Future precipitation changes over
379 China under 1.5 °C and 2.0 °C global warming targets by using CORDEX
380 regional climate models, Sci. Total Environ., 640-641, 543-554, 2018.
- 381 Li, K., Liao, H., Cai, W. J., and Yang, Y.: Attribution of anthropogenic influence on
382 atmospheric patterns conducive to recent most severe haze over eastern China,
383 Geophys. Res. Lett., 45, 2072-2081, 2018.
- 384 Li, Q., Zhang, R. H., and Wang, Y.: Interannual variation of the wintertime fog-haze
385 days across central and eastern China and its relation with East Asian winter
386 monsoon, Int. J. Climatol., 36, 346-354, 2016.
- 387 Liao, H. and Chang, W. Y.: Integrated assessment of air quality and climate change for
388 policy-making-highlights of IPCC AR5 and research challenges, National
389 Science Review, 1(2), 176-179, 2014.
- 390 State Council: *Air pollution prevention and control action plan*. Clean Air Alliance of
391 China Rep., 20 pp., www.cleanairchina.org/product/6349.html, 2013.



- 392 Stott, P. A., Stone, D. A., and Allen, M. R.: Human contribution to the European
393 heatwave of 2003, *Nature*, 432, 610-614, 2004.
- 394 Tang, G. Q., Zhao, P. S., Wang, Y. H., Gao, W. K., Cheng, M. T., Xin, J. Y., Li, X., and
395 Wang, Y. S.: Mortality and air pollution in Beijing: the long-term relationship,
396 *Atmos. Environ.*, 150, 238-243, 2017.
- 397 Tie, X. X., Huang, R. J., Dai, W. T., Cao, J. J., Long, X., Su, X. L., Zhao, S. Y., Wang,
398 Q. Y., and Li, G. H.: Effect of heavy haze and aerosol pollution on rice and wheat
399 productions in China, *Sci. Rep.*, 6, 29612, 2016.
- 400 Wang, H. J.: On assessing haze attribution and control measures in China, *Atmos.*
401 *Oceanic Sci. Lett.*, 11(2), 120-122, 2018.
- 402 Wang, H. J. and Chen, H. P.: Understanding the recent trend of haze pollution in
403 eastern China: roles of climate change, *Atmos. Chem. Phys.*, 16, 4205-4211,
404 2016.
- 405 Wang, H. J., Chen, H. P., and Liu, J. P.: Arctic sea ice decline intensified haze
406 pollution in eastern China, *Atmos. Oceanic Sci. Lett.*, 8, 1-9, 2015.
- 407 Wang, H. J., Sun, J. Q., Chen, H. P., Zhu, Y. L., Zhang, Y., Jiang, D. B., Lang, X. M.,
408 Fan, K., Yu, E. T., and Yang, S.: Extreme climate in China: facts, simulation and
409 projection. *Meteorol. Z.*, 21, 279-304, 2012.
- 410 Wang, X., Dickinson, R., Su, L., Zhou, C., and Wang, K.: PM_{2.5} pollution in China
411 and how it has been exacerbated by terrain and meteorological conditions, *Bull.*
412 *Amer. Meteorol. Soc.*, 99(1), 105-119, 2018.
- 413 World Health Organization: *Air quality guidelines: Global update 2005*. World Health



- 414 *Organization* *Rep.*, 496 pp.,
- 415 www.euro.who.int/_data/assets/pdf_file/0005/78638/E90038.pdf/, 2014.
- 416 Xiao, D., Li, Y., Fan, S. J., Zhang, R. H., Sun, J. R., and Wang, Y.: Plausible influence
417 of Atlantic Ocean SST anomalies on winter haze in China, *Theor. Appl. Climatol.*,
418 122, 249-257, 2015.
- 419 Xu, Y. Y. and Lamarque, J. F.: Isolating the meteorological impact of 21st century
420 GHG warming on the removal and atmospheric loading of anthropogenic fine
421 particulate matter pollution at global scale, *Earth's Future*, 6, 428-440, 2018.
- 422 Yang, Y., Liao, H., and Lou, S. J.: Increase in winter haze over eastern China in recent
423 decades: roles of variations in meteorological parameters and anthropogenic
424 emissions, *J. Geophys. Res. Atmos.*, 121, 13050-13065, 2016.
- 425 Yang, Y., Russell, L. M., Lou, S. J., Liao, H., Guo, J. P., Liu, Y., Singh, B., and Ghan,
426 S. J.: Dust-wind interactions can intensify aerosol pollution over eastern China,
427 *Nature communications*, 8, 15333, 2017.
- 428 Yin, Z. C. and Wang, H. J.: The relationship between the subtropical Western Pacific
429 SST and haze over North-Central North China Plain, *Int. J. Climatol.*, 36,
430 3479-3491, 2016.
- 431 Yin, Z. C., Wang, H. J., and Chen, H. P.: Understanding severe winter haze events in
432 the North China Plain in 2014: roles of climate anomalies, *Atmos. Chem. Phys.*,
433 17, 1641-1651, 2017.
- 434 Yin, Z. C., Wang, H. J., and Yuan, D. M.: Interdecadal increase of haze in winter over
435 North China and the Huang-huai area and the weakening of the East Asia winter



- 436 monsoon (in Chinese), Chin. Sci. Bull., 60, 1395-1400, 2015.
- 437 Zhang, R. H., Li., Q., and Zhang, R. N.: Meteorological conditions for the persistent
438 severe fog and haze event over eastern China in January 2013, Sci. China Earth
439 Sci., 57, 26-35, 2014.
- 440 Zhang, Y., Ding, A. J., Mao, H. T., Nie, W., Zhou, D. R., Liu, L. X., Huang, X., and Fu,
441 C. B.: Impact of synoptic weather patterns and inter-decadal climate variability
442 on air quality in the North China plain during 1980-2013, Atmos. Environ., 124,
443 119-128, 2016a.
- 444 Zhang, Z., Zhang, X., Goog, D., Kim, S., Mao, R., and Zhao, X.: Possible influence of
445 atmospheric circulations over winter haze pollution in the Beijing-Tian-Hebei
446 region, northern China, Atmos. Chem. Phys., 16, 561-571, 2016b.
- 447 Zhao, S., Li, J. P., and Sun, C.: Decadal variability in the occurrence of wintertime
448 haze in central eastern China tied to the Pacific Decadal Oscillation, Sci. Rep., 6,
449 27424, 2016.
- 450 Zhao, S. Y., Zhang, H., and Xie, B.: The effects of El Niño-Southern Oscillation on
451 the winter haze pollution of China, Atmos. Chem. Phys., 18, 1863-1877, 2018.
- 452



453 **Figure captions**

454 **Figure 1. Observed PM_{2.5} pollution conditions over eastern China during the past**

455 **years.** (a) Annual averaged PM_{2.5} concentration ($\mu\text{g}/\text{m}^3$) for the years of 2015-2017.

456 (b) Variations of annual averaged PM_{2.5} concentration (green bars) in Beijing city and

457 the corresponding number of the severe PM_{2.5} pollution days (red bars). The severe

458 pollution days are defined as the daily averaged PM_{2.5} concentration exceeding 75

459 $\mu\text{g}/\text{m}^3$. (c), (d), and (e) are similar to (b), but for the results of Shanghai, Guangzhou,

460 and Chengdu city, respectively.

461 **Figure 2. Plots of future changes of the total PM_{2.5} as well as its associated species**

462 **averaged over eastern China** in terms of the surface concentration ($\mu\text{g}/\text{m}^3$, right axis

463 in red) and column burden (mg/m^2 , left axis in blue) from the simulations of the

464 RCP8.5_FixAerosol2005 experiment. Ensemble variance (1 sigma) for surface

465 concentration is shown in red shadings.

466 **Figure 3. Changes of severe anthropogenic PM_{2.5} pollution days (> 75 $\mu\text{g}/\text{m}^3$)**

467 **across eastern China from the RCP8.5_FixAerosol2005 experiment.** The left panel

468 illustrates the annual averaged severe pollution days in 2006-2015 and the right panel

469 shows changes of the pollution days at the end of the 21st century with respect to

470 2006-2015. Units: days.

471 **Figure 4. Attributable changes of anthropogenic air pollution days to the**

472 **increased greenhouse gases emissions.** (a) Spatial distribution of FAR for the

473 changes of severe PM_{2.5} pollutions (> 75 $\mu\text{g}/\text{m}^3$) at the end of the 21st century over

474 eastern China. (b) Regional averaged relative changes of air pollution days (left axis



475 in red; $> 25 \text{ } \mu\text{g}/\text{m}^3$) and the corresponding variation of FAR (right axis in blue).

476 Ensemble variance (1 sigma) for the relative changes of pollution days is shown in red

477 shadings. (c) is similar to (b), but for the severe PM_{2.5} pollution days. Units: %.

478 **Figure 5. Simulated changes in weather conditions of the air pollutions across**
479 **eastern China due to the GHG-induced warming.** (a) Changes of the planetary
480 boundary layer height (PBLH) at the end of the 21st century with respect to the years
481 of 2006-2015 from the RCP8.5_FixAerosol2005 experiment. (b) and (c) are similar to
482 (a) but for the wind speed at near-surface and 500-hPa levels, respectively. (d)
483 Changes in the light precipitation days (daily accumulated precipitation < 10 mm) at
484 the end of the 21st century with respect to the current state. (e) is similar to (d) but for
485 the heavy precipitation days ($> 10 \text{ mm}$). Units: %.

486 **Figure 6. Changes in the stagnant conditions across China due to the**
487 **GHG-induced warming.** (a) Distribution of the relative changes of the stagnation
488 days at the end of the 21st century against the current state (2006-2015). (b) Variations
489 of the regional averaged stagnation days over eastern China. Ensemble variance (1
490 sigma) is shown in red shadings. (c), (d), (e), and (f) are similar to (b), but for the
491 results of four Chinese economic zones, i.e., JJJ, YRD, PRD, and SC. Units: %.

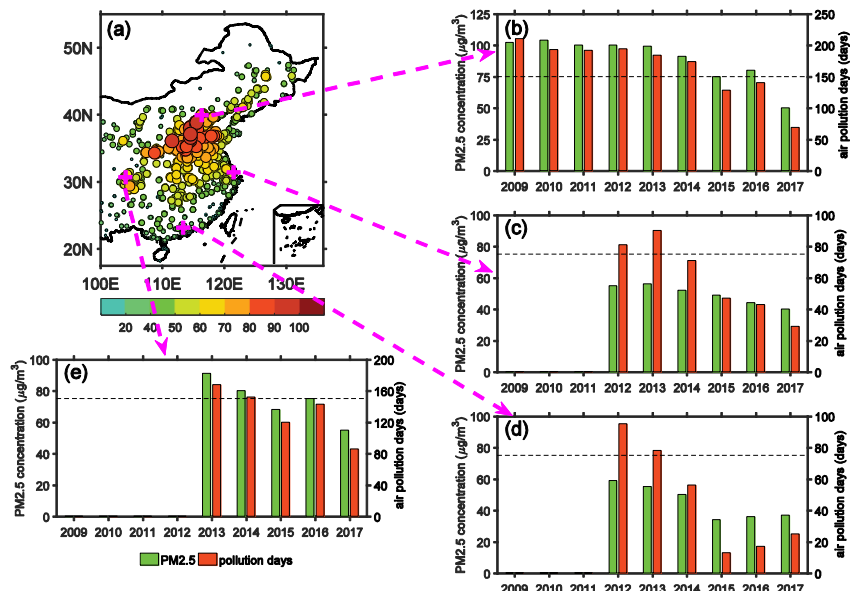
492

493



494 **Figures**

495



496

497 **Figure 1. Observed PM_{2.5} pollution conditions over eastern China during the past**

498 **years. (a)** Annual averaged PM_{2.5} concentration ($\mu\text{g}/\text{m}^3$) for the years of 2015-2017.

499 **(b)** Variations of annual averaged PM_{2.5} concentration (green bars) in Beijing city and

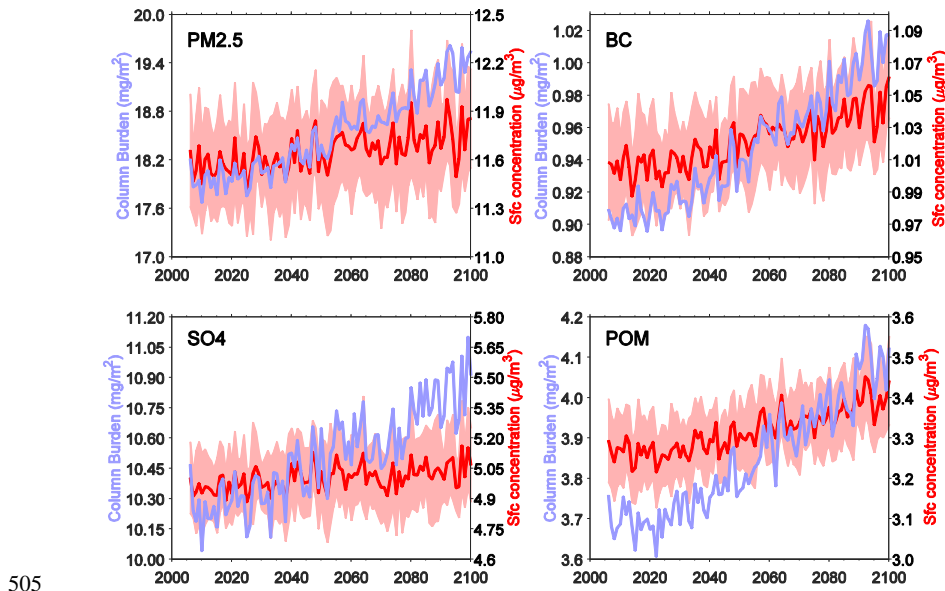
500 the corresponding number of the severe PM_{2.5} pollution days (red bars). The severe

501 pollution days are defined as the daily averaged PM_{2.5} concentration exceeding 75

502 $\mu\text{g}/\text{m}^3$. **(c), (d), and (e)** are similar to **(b)**, but for the results of Shanghai, Guangzhou,

503 and Chengdu city, respectively.

504

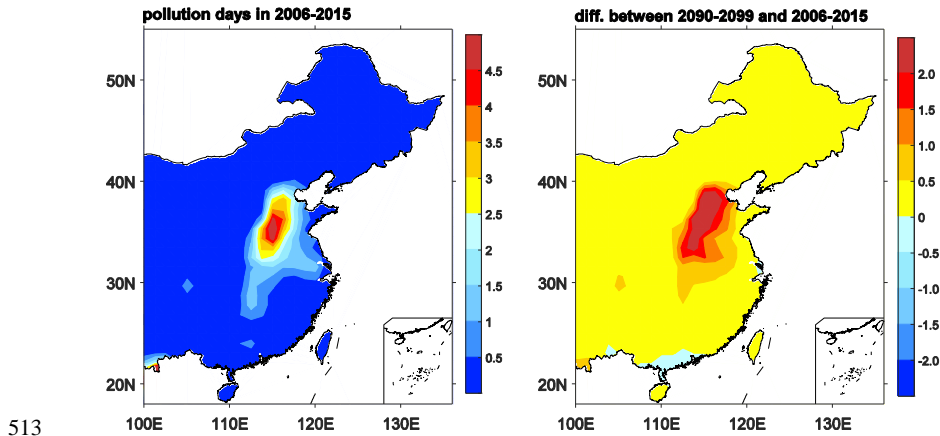


505 **Figure 2. Plots of future changes of the total PM_{2.5} as well as its associated species**

506 **averaged over eastern China** in terms of the surface concentration (µg/m³, right axis
507 in red) and column burden (mg/m², left axis in blue) from the simulations of the
508 RCP8.5_FixAerosol2005 experiment. Ensemble variance (1 sigma) for surface
509 concentration is shown in red shadings.

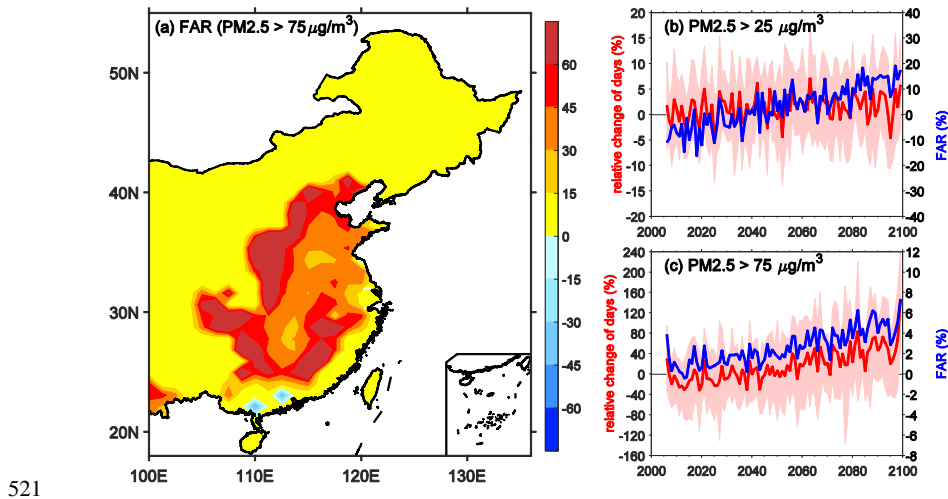
511

512

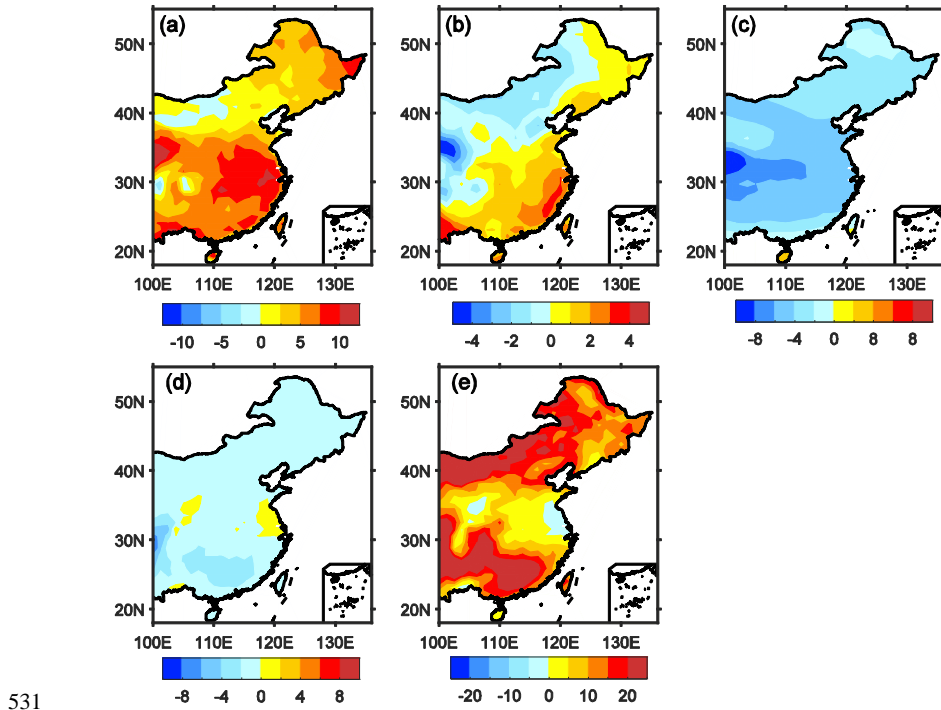


513
514 **Figure 3. Changes of severe anthropogenic PM_{2.5} pollution days (> 75 µg/m³)**
515 **across eastern China from the RCP8.5_FixAerosol2005 experiment.** The left panel
516 illustrates the annual averaged severe pollution days in 2006-2015 and the right panel
517 shows changes of the pollution days at the end of the 21st century with respect to
518 2006-2015. Units: days.

519
520



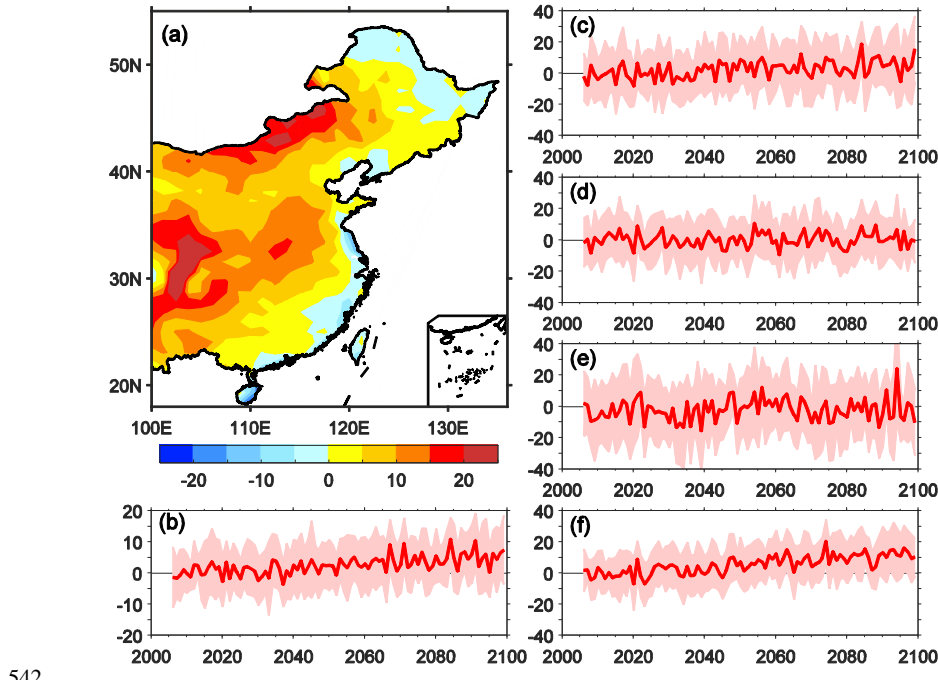
521
 522 **Figure 4. Attributable changes of anthropogenic air pollution days to the**
 523 **increased greenhouse gases emissions.** (a) Spatial distribution of FAR for the
 524 changes of severe PM_{2.5} pollutions ($> 75 \mu\text{g}/\text{m}^3$) at the end of the 21st century over
 525 eastern China. (b) Regional averaged relative changes of air pollution days (left axis
 526 in red; $> 25 \mu\text{g}/\text{m}^3$) and the corresponding variation of FAR (right axis in blue).
 527 Ensemble variance (1 sigma) for the relative changes of pollution days is shown in red
 528 shadings. (c) is similar to (b), but for the severe PM_{2.5} pollution days. Units: %.
 529
 530



531 **Figure 5. Simulated changes in weather conditions of the air pollutions across**
 532 **eastern China due to the GHG-induced warming.** (a) Changes of the planetary
 533 boundary layer height (PBLH) at the end of the 21st century with respect to the years
 534 of 2006-2015 from the RCP8.5_FixAerosol2005 experiment. (b) and (c) are similar to
 535 (a) but for the wind speed at near-surface and 500-hPa levels, respectively. (d)
 536 Changes in the light precipitation days (daily accumulated precipitation < 10 mm) at
 537 the end of the 21st century with respect to the current state. (e) is similar to (d) but for
 538 the heavy precipitation days (> 10 mm). Units: %.

540

541



542

543 **Figure 6. Changes in the stagnant conditions across China due to the**
 544 **GHG-induced warming.** (a) Distribution of the relative changes of the stagnation
 545 days at the end of the 21st century against the current state (2006-2015). (b) Variations
 546 of the regional averaged stagnation days over eastern China. Ensemble variance (1
 547 sigma) is shown in red shadings. (c), (d), (e), and (f) are similar to (b), but for the
 548 results of four Chinese economic zones, i.e., JJJ, YRD, PRD, and SC. Units: %.

549

550